Somatic Cell and Molecular Genetics, Vol. 19, No. 4, 1993, pp. 363–375

Targeting Vector Configuration and Method of Gene Transfer Influence Targeted Correction of the *APRT* Gene in Chinese Hamster Ovary Cells

Rodney S. Nairn,[1] Gerald M. Adair,[1] Thomas Porter,[2] Sandra L. Pennington,[2] Debra G. Smith,[1] John H. Wilson,[2] and Michael M. Seidman[3]

[1]Department of Carcinogenesis, University of Texas M.D. Anderson Cancer Center, Science Park–Research Division, Smithville, Texas 78957; [2]Verna and Marrs McLean Department of Biochemistry, Baylor College of Medicine, Houston, Texas 77030; and [3]Maryland Research Laboratories, Otsuka Pharmaceutical Co., Ltd., Rockville, Maryland 20850

Received 24 May 1993

Abstract—*A 21-bp deletion in the third exon of the* APRT *gene in Chinese hamster ovary (CHO) cells was corrected by transfection with a plasmid containing hamster* APRT *sequences. Targeted correction frequencies in the range of 0.3–3.0 × 10^{-6} were obtained with a vector containing 3.2 kb of* APRT *sequence homology. To examine the influence of vector configuration on targeted gene correction, a double-strand break was introduced at one of two positions in the vector prior to transfection by calcium phosphate-DNA coprecipitation or electroporation. A double-strand break in the region of* APRT *homology contained in the vector produced an insertion-type vector, while placement of the break just outside the region of homology produced a replacement-type vector. Gene targeting with both linear vector configurations yielded equivalent ratios of targeted recombinants to nontargeted vector integrants; however, targeting with the two different vector configurations resulted in different distributions of targeted recombination products. Analysis of 66 independent APRT$^+$ recombinant clones by Southern hybridization showed that targeting with the vector in a replacement-type configuration yielded fewer targeted integrants and more target gene convertants than did the integration vector configuration. Targeted recombination was about fivefold more efficient with electroporation than with calcium phosphate–DNA coprecipitation; however, both gene transfer methods produced similar distributions of targeted recombinants, which depended only on targeting vector configuration. Our results demonstrate that insertion-type and replacement-type gene targeting vectors produce similar overall targeting frequencies in gene correction experiments, but that vector configuration can significantly influence the yield of particular recombinant types.*

INTRODUCTION

Development of gene transfer methods for targeted modification of endogenous genes in mammalian cells has progressed substantially in the past few years (1–10). In addition to practical applications in biotechnology and medicine, study of targeted recombination has potential for elucidating mechanisms of homologous recombination in mammalian cells. Several recent studies (9–13) have focused on the effects of manipulating targeting vector structure for introduction of sequence replacement mutations to inactivate endogenous genes. Results of these studies suggest that the frequency of

0740-7750/93/0700-0363$07.00/0

targeted recombination in mammalian cells depends on the extent of sequence homology between targeting vector and target gene, but may also be influenced by the structure of the targeting vector (11–13).

In previous studies (14, 15), we used targeted recombination to correct a small deletion in exon 5 of the adenine phosphoribosyltransferase (*APRT*) gene in a Chinese hamster ovary (CHO) cell line, ATS-49tg. ATS-49tg is derived from CHO-AT3-2, which has only one *APRT* allele (16) and thus provides a well-suited experimental system for studying targeted gene correction. Analysis of recombinant clones arising from ATS-49tg after targeted correction (14, 15) revealed recombinant *APRT* structures consistent with three classes of recombination events: (1) targeted correction of the deletion in the endogenous *APRT* gene by sequence replacement or gene conversion (target convertants), (2) targeted integration into the chromosomal *APRT* gene (target integrants), and (3) correction of *APRT* sequences in the vector and subsequent random integration of corrected plasmid (vector convertants). Correction of the vector was particularly surprising in one study (14), because the truncated *APRT* sequence in the vector lacked the entire 5′ portion of the gene and contained no homology upstream of the deleted region. We had anticipated that homology on both sides of this large deletion would be required for correction of plasmid *APRT* sequences; however, vector convertants accounted for nearly one-third (9/31) of APRT$^+$ recombinants in this study.

In the present study, we tested the analogous question of whether homology is required on both sides of a double-strand break in the vector for efficient correction of the endogenous target gene by recombination with a targeting vector. Although other recent studies (11–13) have examined similar issues regarding targeted disruption of endogenous genes in mammalian cells, the effects of targeting vector structure on targeted gene correction have not been extensively investigated. In the present study, we used a CHO cell gene transfer recipient containing a different *APRT* deletion than that in ATS-49tg cells to confirm the generality of our previous targeted gene correction results (14, 15). This cell line, U1S-30tg, also has a mutated excision repair cross-complementing 2 (*ERCC2*) gene, allowing us to test whether this particular DNA repair gene mutation would influence targeted recombination. Finally, we compared two different, widely used methods of gene transfer, calcium phosphate–DNA coprecipitation and electroporation, to assess the influence of gene transfer method on targeted gene correction. Our results indicate that electroporation was a more efficient avenue of gene transfer for targeted correction of *APRT* than calcium phosphate transfection. The linear configuration of the vector in our gene targeting experiments influenced the distribution, but not the overall frequency, of targeted recombination events, and this effect was independent of the method of gene transfer.

MATERIALS AND METHODS

Cell Lines and Culture Conditions. The APRT-deficient CHO cell line U1S-30 was derived from CHO cell line UVL-1 (17) by selection for spontaneous 8-azaadenine resistance as previously described (18, 19). U1S-30 cells are hemizygous at the *APRT* locus, containing a single, mutationally inactivated copy of the *APRT* gene with an MspI restriction fragment polymorphism that reflects loss of the exon 3 MspI restriction site (Fig. 1). We have been unable to obtain spontaneous APRT$^+$ revertants from this cell line. For the experiments described here, a spontaneous hypoxanthine–guanine phosphoribosyltranferase (*HPRT*) -deficient subclone of U1S-30 (U1S-30tg) was selected in 6-thioguanine (18, 19). Cells were cultured as

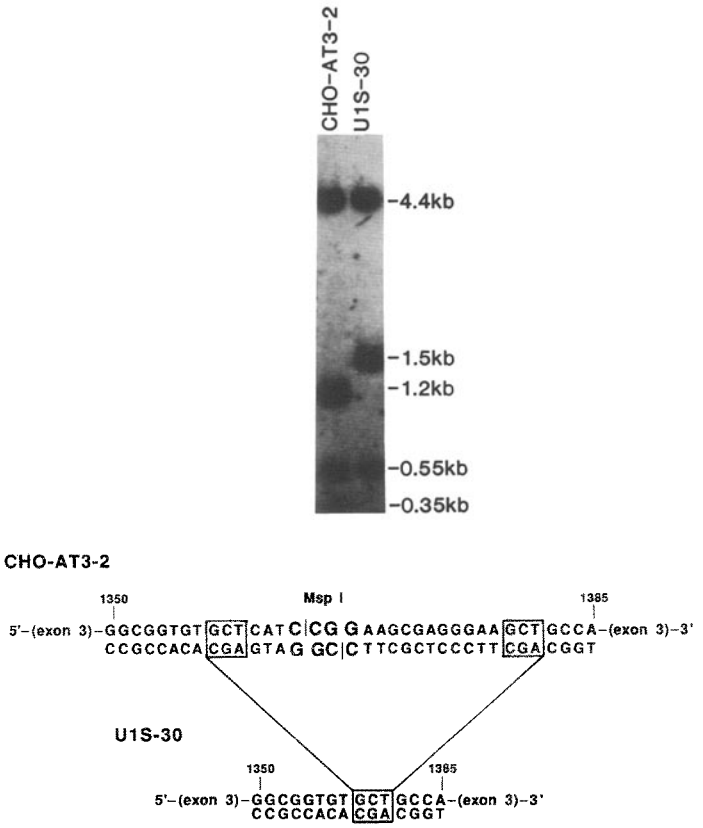

Fig. 1. MspI restriction fragment length polymorphism in U1S-30 cells resulting from a 21-bp deletion in the hamster wild-type *APRT* gene. Restriction digestion fragment patterns resulting from Southern blots of MspI-digested cellular DNA from CHO cell lines CHO-AT3-2 (wild-type) and U1S-30 probed with a 3.9-kb BamHI fragment containing the entire hamster *APRT* gene are shown at the top. The loss of wild-type 1.2- and 0.35-kb fragments and the appearance of a novel 1.5-kb fragment is due to a 21-bp deletion in U1S-30 cells as shown at the bottom. The characteristics of the deletion were determined by direct sequencing of PCR- amplified DNA as described in the text.

monolayers in alpha-modified minimal essential medium (α-MEM) supplemented with 10% fetal calf serum (FCS), penicillin (50 units/ml), and streptomycin (50 μg/ml) at 37°C in a humidified atmosphere of 5% CO_2–95% air. Selections for GPT^+ phenotype in hypoxanthine–amethopterin–thymidine (HAT) and for $APRT^+$ phenotype in alanosine–azaserine–adenine (ALASA) media were performed as previously described (14). Alanosine (NSC-529469) was a gift of the Drug Synthesis and Chemistry Branch of the National Cancer Institute.

PCR Amplification and Direct Sequencing. A genomic DNA fragment containing the exon 3 region of the U1S-30 *APRT* gene was amplified by the polymerase chain reaction, essentially as described by Saiki et al. (20) using the GeneAmp DNA Amplification kit (Perkin-Elmer/Cetus). One microgram of purified genomic DNA was added to a reaction mixture that included 1 μM of forward and reverse amplification primers (20-mers), deoxyribonucleotide triphosphates at 200 μM each, and 1.25 units of AmpliTaq DNA polymerase, in a total volume of 50 μl. DNA amplifications were performed in a Perkin-Elmer/Cetus DNA thermal cycler for 15 cycles with denaturation for 1 min at 94°C, annealing for 1 min at 50°C, and extension

for 1 min at 70°C, followed by 15 cycles in which the extension step was increased to 2 min. Following chloroform extraction and purification through a Centricon 30 filter (Amicon), the amplification product was sequenced using the TaqTrack Sequencing kit (Promega) with an internal sequencing primer. Cycling times were as described by Carouthers et al. (21). Samples were electrophoresed in 8 M urea, 6% polyacrylamide gels, which were dried and subjected to autoradiography.

Plasmid DNA. Plasmid pAG100 (Fig. 2) was derived from pAG1 (22) and contains hamster *APRT* sequences from an EcoRV site in the second exon to a BamHI site in genomic hamster DNA located ~1.4 kb downstream from the *APRT* polyadenylation signal. This plasmid also contains the *GPT* transcription cassette from pSV2gpt (23).

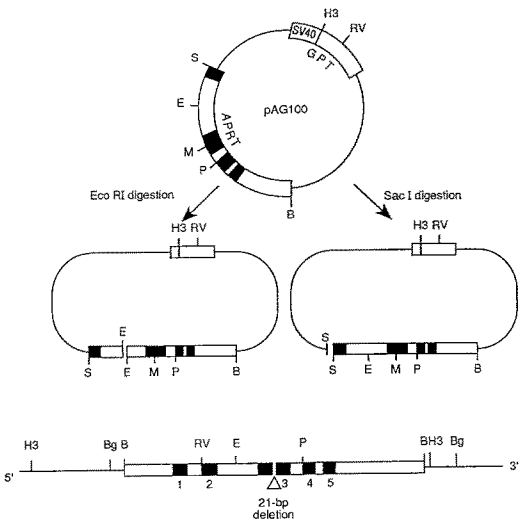

Fig. 2. Structures of EcoRI- and SacI-digested plasmid pAG100 and the U1S-30tg *APRT* locus. Plasmid pAG100 contains wild-type hamster *APRT* sequences from exon 2 through exon 5 as shown (exons are shown as black boxes). Transfection with pAG100 digested with EcoRI presents a vector with *APRT* homology on both sides of a double-strand break, whereas SacI-digested pAG100 has *APRT* homology on only one side of the break. At the bottom of the figure, the location of the 21-bp deletion in exon 3 is shown in the target gene, the U1S-30tg chromosomal *APRT* locus. Restriction enzyme sites shown are: B, BamHI; Bg, BglII; E, EcoRI; H3, HindIII; M, MroI; P, PstI; RV, EcoRV; S, SacI.

Plasmid pAG100 was derived from pAG1 in several steps involving intermediate plasmids, using conventional cloning methods (24); construction of pAG100 resulted in the replacement of the EcoRV site in exon 2 of *APRT* with a unique SacI site. Plasmid DNA for transfections was prepared from cleared lysates on CsCl isopycnic gradients (25). Prior to transfections, linear plasmids were purified by phenol extraction and ethanol precipitation after treatment of EcoRI- or SacI-digested DNA with proteinase K (200 μg/ml) in 0.1% SDS, 1 M lithium acetate at 37°C for 2 h.

Gene Transfer Methods. Gene transfer by calcium phosphate transfection was modified from methods previously described (26, 27), without using carrier DNA. U1S-30tg cells cultured in 100-mm petri dishes (1.2×10^6 per dish) were exposed to 8 μg (each dish) of plasmid DNA–calcium phosphate precipitate, then shocked for 25 min with 10% dimethylsulfoxide in culture medium and replenished with fresh culture media. Cells were detached by treatment with trypsin–EDTA after 40–42 h and plated into HAT and ALASA selection. Nontargeted, GPT^+ colonies were selected by plating a small aliquot of the total population of harvested cells to HAT dishes. Targeted recombinants ($APRT^+$ clones) were selected after plating ~80% of the population to ALASA dishes. After 12–14 days, colonies were scored and some were cloned and expanded for analysis of cellular DNA by Southern blotting as previously described (14).

Electroporation was performed using a BioRad GenePulser electroporator. Exponentially growing cells were harvested by centrifugation after detachment of cells with trypsin–EDTA and resuspended at 2×10^7 cells/ml in sterile, ice-cold electroporation buffer consisting of 272 mM sucrose, 7 mM $NaH_2PO_4 \cdot 7H_2O$, 1 mM Mg_2Cl, and plasmid DNA (10 μg/ml). Electroporation of 0.85 ml of resuspended cells in 0.4-cm cuvettes was

conducted at 500 V, 25 μFD (time constant approximately 4.5). After electroporation, cells were held for exactly 10 min on ice, diluted in ice-cold medium, and plated to α-MEM (six plates per cuvette). Forty hours later, cultures were trypsinized and plated to selection media (HAT and ALASA) as for calcium phosphate transfections. Frequencies were calculated based on the total number of GPT^+ and $APRT^+$ clones, corrected for dilutions prior to plating in selection media. Only one $APRT^+$ clone per independent regime was used in subsequent Southern analysis of recombinants; an independent regime was represented by each original plate in calcium phosphate experiments, or by each of the six plates arising from a single cuvette in electroporations.

Southern Blot Analysis. Southern blot hybridization analysis was performed on DNA samples isolated from recombinant clones using previously described methods of DNA purification (14, 26, 27). After digestion with restriction endonucleases and electrophoresis in 0.8% agarose gels, DNA samples were transferred to either nitrocellulose or charged nylon (NEN GeneScreen Plus or Oncor SureBlot) membranes by capillary blotting. Hybridization probes were labelled with [^{32}P]dCTP by nick translation (28) or random-prime labeling methods (29). Conditions of hybridization and washing for nitrocellulose membranes have been described (14, 26); hybridization, washing, and stripping procedures for reprobing of GeneScreen Plus and SureBlot membranes followed manufacturers' instructions. In some cases BspMII or BspEI isoschizomers of MroI, instead of this enzyme, were used in DNA digestions for Southern blots.

RESULTS

Effects of Vector Configuration and Transfection Method on APRT *Targeted Correction Frequencies.* Double-strand breaks are known to stimulate extrachromosomal homologous recombination in mammalian cells (30–32) and may also promote targeted recombination (4, 10, 33, 34). In previous studies (14, 15), we used linear targeting vectors with *APRT* homology on both sides of a double-strand break to correct a deletion in the endogenous *APRT* gene of transfected cells by homologous recombination. To test whether homology on both sides of a double-strand break in vector DNA was required for efficient correction of the *APRT* locus, we transfected U1S-30tg cells with pAG100 in two different linear configurations. As shown in Fig. 2, EcoRI cleavage of pAG100 results in *APRT* homology on both sides of a double-strand break, producing an insertion-type targeting vector, whereas cleavage with SacI leaves *APRT* homology on only one side of the break, producing a replacement-type vector. Transfection with pAG100 in either linear configuration results in targeted correction of the *APRT* deletion in U1S-30tg, giving rise to $APRT^+$ clones. Random vector integrations resulting from nonhomologous recombination (i.e., nontargeted integrants) are GPT^+ and can be selected by growth in HAT medium. Data for frequencies of both targeted and nontargeted recombination in pAG100 experiments are presented in Table 1. Transfection by calcium phosphate–DNA coprecipitation with EcoRI-digested pAG100 (insertion-type vector configuration) produced targeted recombinants at a frequency of 3×10^{-7} and nontargeted integrants at a frequency of 2.2×10^{-3}. In a previous study in which we used calcium phosphate transfection with a similar insertion-type vector to correct a different *APRT* deletion (14), we observed similar frequencies for targeted correction (4.1×10^{-7}) and random integration (1.6×10^{-3}). Electroporation of pAG100 in an insertion-type configuration produced nontargeted integrants at a comparable frequency (2.7×10^{-3}), but the frequency of targeted correction was fivefold higher (1.5×10^{-6}).

Table 1. Frequencies of Targeted Correction Events and Nontargeted Integrations in U1S-30tg Cells

	Total number of cells transfected	Frequencies		
		GPT^+	$APRT^+$	Ratio[a]
EcoRI-digested pAG100 (insertion vector)				
Calcium phosphate	1.2×10^8	2.2×10^{-3}	0.3×10^{-6}	1/7300
Electroporation	0.7×10^8	2.7×10^{-3}	1.5×10^{-6}	1/1800
SacI-digested pAG100 (replacement vector)				
Calcium phosphate	1.2×10^8	4.9×10^{-3}	0.7×10^{-6}	1/7000
Electroporation	1.7×10^8	5.1×10^{-3}	3.2×10^{-6}	1/1600

[a]Ratio of targeted recombination to nontargeted vector integration (i.e., $APRT^+$ frequency/GPT^+ frequency).

Transfection of U1S-30tg cells with SacI-digested pAG100 (replacement-type vector configuration) showed the same five-fold increase in targeted correction when the DNA was introduced by electroporation (Table 1). Transfections using this vector configuration by either calcium phosphate–DNA coprecipitation or electroporation resulted in somewhat higher frequencies for both targeted and nontargeted events relative to insertion-type vector configuration (Table 1). The presence of a second marker (*GPT*) in the targeting vector allows targeted correction frequencies to be normalized to nontargeted integration frequencies; thus, the ratios in Table 1 represent the relative efficiencies of targeted recombination. The difference in absolute frequencies for the two different vector configurations in both calcium phosphate transfection and electroporation experiments is unexplained; however, the ratios of targeted to nontargeted frequencies were very similar for both insertion-type and replacement-type vector configurations, when introduced by the same transfection method (Table 1). The fact that these ratios were constant regardless of vector configuration indicates that the configuration of the vector (i.e., insertion-type vs. replacement-type) did not affect the efficiency of targeted correction of the *APRT* locus in U1S-30tg cells. We suspect that the difference in absolute frequencies we observed results from some variability introduced by the preparation of plasmid DNA or cells prior to transfection.

Effects of Vector Configuration on Distribution of Targeted Correction Events. The target mutation in U1S-30tg cells was a spontaneous deletion that resulted in loss of an MspI site in exon 3 of the single-copy, endogenous *APRT* gene. PCR amplification and direct sequencing revealed that the U1S-30tg *APRT* allele contained a 21-bp deletion in exon 3 (Fig. 1). As a consequence of this deletion, the wild-type 1.2-kb MspI *APRT* fragment has been replaced in U1S-30tg by a 1.5-kb MspI fragment, making the U1S-30tg target and wild-type (i.e., corrected) sequences easily distinguishable by Southern blotting (see Fig. 1). This 4-bp MspI site is contained within a 6-bp MroI site, which is also lost due to the deletion.

To analyze the distribution of *APRT* targeted correction events, we subjected $APRT^+$ clones to Southern blot analysis after digestion with MroI and HindIII restriction enzymes. Figure 3 shows diagnostic restriction fragments expected at the U1S-30tg *APRT* locus after targeted correction with pAG100 leading to target gene conversion or vector integration at the target gene; Fig. 4 shows Southern blots with examples of targeted recombinants. The fragments illustrated in Fig. 3 are observed using a hybridization probe consisting of sequences from the BamHI site located 5′ to *APRT* extending downstream to the EcoRV site in

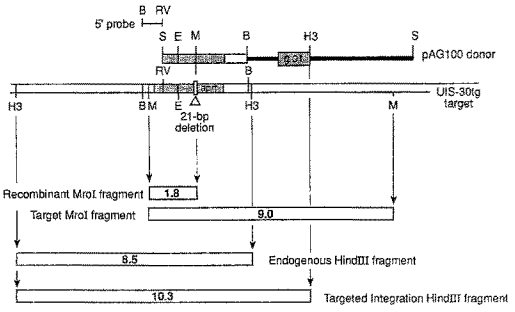

Fig. 3. Restriction fragment patterns for U1S-30tg *APRT* recombinants. The structures of plasmid pAG100 and the endogenous U1S-30tg *APRT* locus are shown, with restriction fragments generated from target locus correction and targeted integration recombination products illustrated. Restriction enzyme sites follow abbreviations used in Fig. 2.

exon 2; this 600-bp fragment is absent from pAG100 and will not detect vector sequences unless they are linked to the endogenous fragment corresponding to this probe. As illustrated in Fig. 3, digestion of DNA from U1S-30tg generates a 9-kb MroI fragment and a 8.5-kb HindIII fragment, which each contain the 21-bp deletion in exon 3 (Fig. 4, lanes 1). In all targeted recombinants, a 1.8-kb MroI fragment will result from linkage of the MroI site at the 5′ end of the gene to the MroI site in exon 3, which is donated by pAG100. In targeted recombinants arising from sequence replacement at the U1S-30tg *APRT* locus (target convertants), the 9-kb MroI fragment will be replaced by the 1.8-kb MroI fragment, but the endogenous 8.5-kb HindIII fragment will be unchanged (Fig. 4, lanes 2, 3, 4, 7). Recombinants arising from targeted integration of the vector at the U1S-30tg *APRT* target locus (target integrants) will lose the 8.5-kb endogenous HindIII fragment in addition to the 9-kb MroI fragment and gain a new 10.3-kb HindIII fragment (Fig. 4, lanes 6). Recombinants arising from correction of the deletion in the vector (vector convertants) will retain both the 9-kb MroI and 8.5-kb HindIII

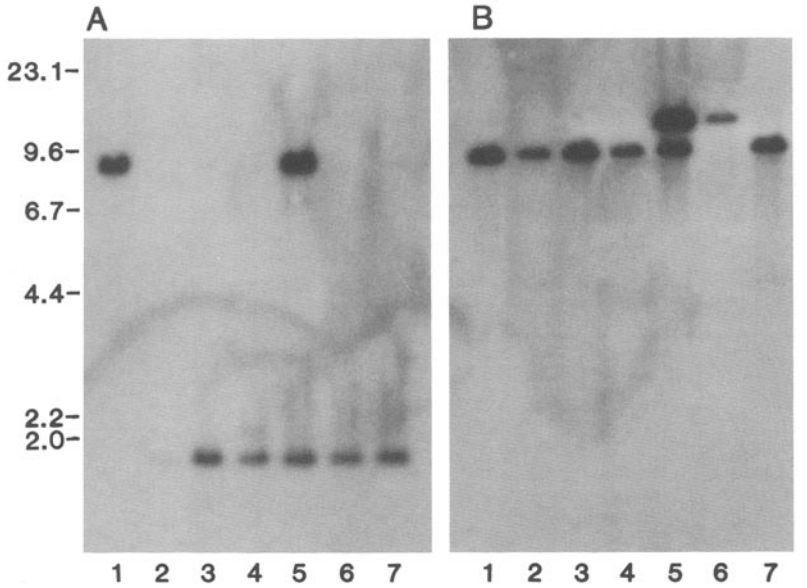

Fig. 4. Southern blot analysis of MroI- and HindIII-digested DNA samples from APRT$^+$ recombinant clones. Membranes were probed with the ^{32}P-labeled 600-bp BamHI–EcoRV *APRT* fragment shown at the top of Fig. 3. (A) MroI (BspEI) digests: lane 1 is U1S-30tg DNA, lanes 2–7 are DNA samples from recombinants. (B) HindIII digests: lanes are the same as for A. Lanes 2–4 and 7 are DNA samples from clones arising from target gene correction events (i.e., target convertants); lane 5 is DNA from a vector convertant, and lane 6 is from a target integrant.

fragments characteristic of the parental cell line, but will also have the diagnostic 1.8-kb MroI fragment (Fig. 4, lanes 5). HindIII-digested DNA from vector convertants will show another band arising from random integration in addition to the 8.5 kb fragment derived from the target locus (Fig. 4B, lanes 5).

To determine if vector configuration influenced the distribution of targeted correction events, we used the criteria described above to analyze 66 independent APRT$^+$ clones from pAG100-transfected cells; 26 clones were from transfections with EcoRI-digested pAG100 (insertion-type configuration) and 40 clones were from SacI-digested pAG100 (replacement-type configuration). The results of Southern blot analysis of DNA samples from these APRT$^+$ recombinant clones are shown in Table 2. These data indicate that transfection with the vector in replacement-type configuration yielded significantly fewer targeted integrants (3/40) than did transfection with the vector in insertion-type configuration (9/26). In addition, the proportion of target convertants at the U1S-30tg *APRT* locus was increased using replacement-type vector (28/40) compared to the insertion-type vector (11/26). The proportions of vector convertants were nearly the same for both vector configurations.

Results presented in Table 2 also show that the transfection method did not significantly influence the distribution of targeted recombination events. Targeted recombinants arising from SacI-digested pAG100 transfections showed an almost identical distribution for both calcium phosphate and electroporation methods. For EcoRI-digested pAG100-derived recombinants, there was a small apparent increase in the proportion of target convertants arising from calcium phosphate transfection (7/14) compared to electroporation (4/12). Given the small sample size, this difference is probably not significant; however, similar differences are apparent in comparing these results with results of previous studies using other insertion-type vectors for targeted correction of the CHO *APRT* locus (14, 15). In these experiments, calcium phosphate transfection with an insertion-type vector (14) resulted in the distribution: target convertants (16/31), target integrants (6/31), vector convertants (9/31). In separate experiments (15), electroporation of the same cell line, ATS-49tg, with a second insertion-type vector gave the distribution: target convertants (17/51), target integrants (16/51), vector convertants (18/51). Overall, these results indicate that, unlike vector configuration, transfection method did not markedly affect the distribution of targeted recombinants.

APRT *Recombinant Structures in Target Integrant and Vector Convertant Clones.* APRT$^+$ recombinants were classified as target integrants based on replacement of the endogenous 8.5-kb HindIII fragment with a diagnostic 10.3-kb fragment generated

Table 2. Distribution of Targeted Correction Events at *APRT* Locus of U1S-30tg Cells

	Target convertant	Target integrant	Vector convertant
EcoRI-digested pAG100 (insertion vector)			
Calcium phosphate	7/14	4/14	3/14
Electroporation	4/12	5[a]/12	3/12
	11/26 (42%)	9/26 (35%)	6/26 (23%)
SacI-digested pAG100 (replacement vector)			
Calcium phosphate	14/20	2/20	4/20
Electroporation	14/20	1/20	5/20
	28/40 (70%)	3/40 (8%)	9/40 (23%)

[a]Blot analysis of one clone indicated the presence of original *APRT* gene target linkages in addition to both 10.3-kb and 5.8-kb diagnostic targeted integration fragments in HindIII digests; this clone was classified as a target integrant because it is highly improbable that both diagnostic HindIII fragments would be present in a vector convertant.

by linkage of the HindIII site in pAG100 with an endogenous HindIII site 5′ to the *APRT* gene (see Fig. 3). Targeted integration of vector DNA into the *APRT* gene results in a partial duplication of *APRT* sequences, with 3.2 kb of *APRT* sequence from vector DNA located 3′ to the reconstructed *APRT* gene and the integrated *GPT* sequence. This recombinant structure generates another HindIII restriction linkage diagnostic for target integrants, a 5.8-kb fragment that represents the linkage of the vector HindIII site to the downstream chromosomal HindIII site that defines the 3′ boundary of the endogenous 8.5-kb fragment. The 600-bp BamHI–EcoRV *APRT* fragment used as the hybridization probe for the blots of Fig. 4 (this probe is shown in Fig. 3) will not detect this downstream HindIII fragment, since its corresponding sequence is missing. However, probing with the 3.9-kb BamHI fragment containing the entire *APRT* gene will reveal both diagnostic HindIII fragments in target integrants.

Figure 5 shows the blot of Fig. 4B stripped and reprobed with a radiolabeled 3.9-kb BamHI fragment, revealing both diagnostic HindIII fragments in DNA from a target integrant (Fig. 5, lane 6). Vector convertants (e.g., Fig. 5, lane 5) are distinguished from target integrants (e.g., Fig. 5, lane 6) in lacking the 5.8-kb diagnostic HindIII fragment detected by the 3.9-kb probe, as well as possessing the endogenous 8.5-kb fragment. In the case of the vector convertant in Fig. 5 (lane 5), the 10.3-kb HindIII fragment is also present. This 10.3-kb HindIII fragment was observed in 11/15 vector convertants. In these clones, correction of vector DNA has apparently resulted in the transfer of at least 4.5 kb of upstream chromosomal sequence (i.e., to at least the HindIII site ~4.5 kb upstream of the *APRT* gene) to the vector prior to its integration elsewhere in the genome. The additional band in lane 5 indicates an additional, nontargeted vector integration in this clone, which is detected by the 3.9-kb, but not the 600-bp, *APRT* probe.

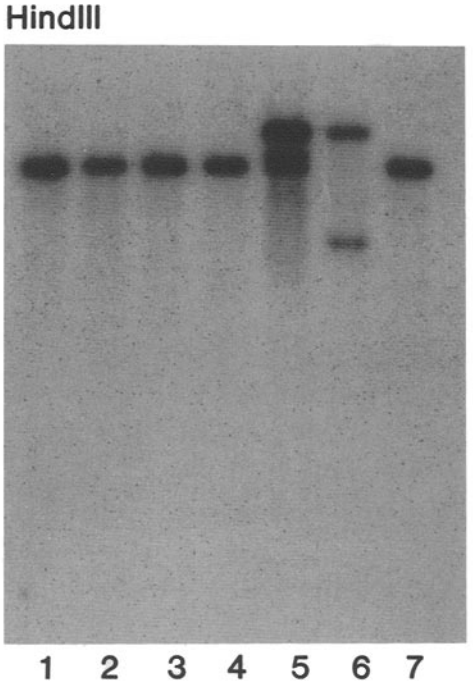

Fig. 5. Southern blot analysis of HindIII-digested DNA samples from APRT$^+$ recombinant clones probed with the 3.9-kb BamHI *APRT* fragment. The membrane of Fig. 4B was stripped and reprobed with the ^{32}P-labeled 3.9-kb BamHI fragment containing the entire *APRT* gene. Lanes are the same as for Fig. 4.

DISCUSSION

In this study, we compared the efficiencies of two different methods of gene transfer, calcium phosphate–DNA coprecipitation and electroporation, in targeted gene correction of the CHO *APRT* locus. Electroporation of pAG100 in two different linear configurations increased the efficiency of targeted correction about fivefold compared to calcium phosphate transfection. This is reflected in the ratios of frequencies of targeted recombination events to nontargeted vector integrations, presented in Table 1. Several factors could contribute to the

apparent difference in efficiencies of targeted recombination between the two transfection methods. Exposure of cells to calcium phosphate–DNA precipitates could influence targeting efficiency by perturbing intracellular levels of Ca^{2+}, which is a potent second messenger. Furthermore, the damaging effects of a particular gene transfer method on transfected DNA or the cells themselves might be an important factor. In this study, we used standard calcium phosphate and electroporation transfection methods and can not rule out that modifications to these methods might further alter the ratios of targeted to nontargeted gene correction frequencies.

This study also examined the effects of targeting vector configuration (i.e., replacement-type vs. insertion-type) on the frequency of targeted correction of *APRT* and on the distribution of recombinants among different classes of recombination events. In our experiments, replacement-type and insertion-type configuration of the targeting vector was determined solely by the position of the double-strand break in the vector, and there were no other differences between the two targeting vector types (see Fig. 2). Results of Table 1 indicate that transfection with the targeting vector in the two different configurations gave very similar efficiencies of targeted correction when targeted recombination frequencies were normalized to frequencies of nontargeted integrations, regardless of the method of gene transfer. In other gene targeting studies, two similar comparisons of insertion and replacement vector configurations in *HPRT* gene disruption experiments in mouse ES cells reached contradictory conclusions. In one study (35), no difference in targeting efficiency was observed, while in a second study (11) insertion-type vectors were apparently up to ninefold more efficient than replacement vectors. A recent study by Deng and Capecchi (13) using 22 different sequence replacement and insertion vectors targeted to the *HPRT* locus in mouse ES cells showed that replacement-type and insertion-type targeting vectors were equally efficient at targeted disruption of this locus, although anomalously low targeting frequencies were observed with certain vectors. These vectors apparently produced low targeting frequencies because of heterologies between vector and target gene sequences at critical positions, not because of vector configuration per se (13). Our targeted gene correction results at the CHO *APRT* locus are thus in general agreement with the conclusions reached by Deng and Capecchi (13) for targeted disruption at the mouse *HPRT* locus.

The insertion vector configuration of the EcoRI-digested pAG100 vector used in the present study is similar to that of insertion-type vectors used in our previous targeted correction experiments at the CHO *APRT* locus (14, 15). In these vectors, the double-strand break is within the region of *APRT* sequence homology in the vector, with homology to the target locus on both sides of the break. Such a targeting vector structure, with homologous DNA in "ends-in" configuration, presumably would allow either or both homologous arms flanking the double-strand break to interact with the target gene and could serve as a substrate for several types of recombination events. These include, as we showed previously (14, 15), targeted correction of the endogenous locus, targeted integration of plasmid sequences at the endogenous locus, and generation of a functional *APRT* gene by correction of vector-borne *APRT* sequences. The relative proportions of these three types of recombination events in the present study using an insertion-type vector to correct the exon 3 *APRT* deletion in U1S-30tg cells (Table 2) were similar to those previously obtained using insertion-type vectors to correct an exon 5 *APRT* deletion in ATS-49tg cells (14, 15).

Although all three types of recombination events were represented among the

targeted recombinants generated by the replacement-type vector used in this study, SacI-digested pAG100, the distribution of recombinants was substantially different from that generated by the insertion-type vector configuration of EcoRI-digested pAG100 (Table 2). When compared directly to EcoRI-digested pAG100, transfection with SacI-digested pAG100 resulted in fewer target integrants and more target convertants, while vector convertants remained about the same. In the case of an insertion-type vector, targeted integration can arise by a single crossover at the site of the double-strand break within the region of *APRT* homology in the vector; however, no analogous pathway for a linear vector monomer in replacement-type configuration would lead to targeted integration by a single crossover. Therefore, a decrease in target integrants with the replacement-type vector was not unexpected and is consistent with the double-strand break repair model largely developed from studies of homologous recombination in *Saccharomyces cerevisiae* (36). Furthermore, the three target integrants observed in our experiments with SacI-cut pAG100 could have arisen by single-reciprocal exchange with a recircularized vector or by recombination with concatamerized vector molecules, as suggested to explain analogous integration recombinants arising from targeted recombination of replacement-type vectors at the *HPRT* locus in mouse ES cells (11). Thus, our result that targeted correction of *APRT* with an insertion vector generated targeted integration recombinants more efficiently than the replacement-type vector we used is consistent with the double-strand break repair model. However, it is also likely that multiple pathways generate targeted recombinants in mammalian cells (14), and pathway utilization could depend on a variety of factors including, but not limited to, targeting vector structure.

Transfection with pAG100 in the two different targeting configurations yielded very similar proportions of vector convertants (Table 2). Since both vector configurations contained only a 3′ segment of the *APRT* gene, correction of vector required the transfer of 5′ *APRT* sequences from the chromosome to plasmid DNA. Analysis of vector convertants showed that 11/15 picked up at least 4.5 kb of chromosomal sequences upstream from the *APRT* gene prior to integration elsewhere in the genome (e.g., Fig. 4, lane 5). It is possible that transfer of chromosomal information to vector could have occurred by intermolecular recombination between vector DNA and an extrachromosomal copy of *APRT* sequences, perhaps in the form of small polydisperse circular DNA (37, 38). Alternatively, vector molecules could pick up missing *APRT* sequences by invading the chromosome through its *APRT* homology and priming DNA synthesis to copy the upstream *APRT* sequences, as we previously suggested (14). The priming of DNA synthesis after homologous pairing is an integral feature of the double-strand break repair model for homologous recombination (36), which has significant experimental support as the primary mechanism for targeted recombination in mammalian cells (4, 10, 12, 15). Other mechanisms not requiring free homologous ends, however, are possible, and further studies will be necessary to define the major pathways for formation of vector convertants in targeted recombination experiments in mammalian cells. This type of recombinant is very common in our targeted correction experiments at the CHO *APRT* locus, and understanding its formation may account for observations in other studies that have reported targeted recombinants in which vector is correctly linked to chromosomal sequences at one end but aberrantly linked at the other end (10, 39, 40).

The CHO cell line used in this study, U1S-30tg, has a mutation in the *ERCC2* DNA repair gene, which is homologous to the *RAD3* gene of yeast (41). Since some

mutations in *RAD3,* which encodes a DNA helicase (42), can lead to pleiotropic effects on mutability and recombination in yeast (43), we were interested in the effect of the *ERCC2* mutation on gene targeting in U1S-30tg cells. Comparison of the results of this study with previous targeting experiments in a CHO cell line carrying a wild-type *ERCC2* gene (14, 15) indicate that there were no significant differences in targeting efficiencies or distribution of recombinants produced by transfection with insertion vectors. A recent study of extrachromosomal recombination confirms that the *ERCC2* mutation in U1S-30 cells does not cause a significant recombination deficiency, although a difference from wild-type CHO cells was observed in UV stimulation of extrachromosomal recombination (44). However, it is possible that this or other *ERCC2* mutations could exert subtle effects on homologous recombination, such as altering the efficiency of the repair of mismatches in heteroduplex recombination intermediates. Whether or not other mutations in the *ERCC2* gene influence targeted recombination in mammalian cells is an interesting question, open to further investigation.

ACKNOWLEDGMENTS

We wish to thank Rita Svensson, Cindy Christmann, and Susan Plaza for excellent technical assistance and Judy Ing and John Riley for assistance with photography and artwork. This work was supported by U.S. Public Health Service grant CA-36361 (R.S.N.), and also by U.S.P.H.S. grants CA-28711 (G.M.A.) and GM-38219 (J.H.W.), from the National Institutes of Health.

LITERATURE CITED

1. Smithies, O., Gregg, R.G., Boggs, S.S., Koralewski, M.A., and Kucherlapati, R. (1985). *Nature* **317**:230–234.
2. Thomas, K.R., and Capecchi, M.R. (1987). *Cell* **51**:503–512.
3. Doetschman, T., Gregg, R.G., Maeda, N., Hooper, M.L., Melton, D.W., Thompson, S., and Smithies, O. (1987). *Nature* **330**:576–578.
4. Jasin, M., and Berg, P. (1988). *Genes Dev.* **2**:1353–1363.
5. Mansour, S.L., Thomas, K.R., and Capecchi, M.R. (1988). *Nature* **336**:348–352.
6. Sedivy, J.M., and Sharp, P.A. (1989). *Proc. Natl. Acad. Sci. U.S.A.* **86**:227–231.
7. Ellis, J., and Bernstein, A. (1989). *Mol. Cell. Biol.* **9**:1621–1627.
8. Capecchi, M.R. (1989). *Science* **244**:1288–1292.
9. Hasty, P., Ramirez-Solis, R., Krumlauf, R., and Bradley, A. (1991). *Nature* **350**:243–246.
10. Valancius, V., and Smithies, O. (1991). *Mol. Cell. Biol.* **11**:1402–1408.
11. Hasty, P., Rivera-Perez, J., Chang, C., and Bradley, A. (1991). *Mol. Cell. Biol.* **11**:4509–4517.
12. Hasty, P., Rivera-Perez, J., Chang, C., and Bradley, A. (1992). *Mol. Cell. Biol.* **12**:2464–2474.
13. Deng, C., and Capecchi, M.R. (1992). *Mol. Cell. Biol.* **12**:3365–3371.
14. Adair, G.M., Nairn, R.S., Wilson, J.H., Seidman, M.M., Brotherman, K.A., MacKinnon, C., and Scheerer, J.B. (1989). *Proc. Natl. Acad. Sci. U.S.A.* **86**:4574–4578.
15. Pennington, S.L., and Wilson, J.H. (1991). *Proc. Natl. Acad. Sci. U.S.A.* **88**:9498–9502.
16. Adair, G.M., Stallings, R.M., Nairn, R.S., and Siciliano, M.J. (1983). *Proc. Natl. Acad. Sci. U.S.A.* **80**:5961–5964.
17. Busch, D., Greiner, C., Lewis, K., Ford, R., Adair, G., and Thompson, L. (1989). *Mutagenesis* **4**:349–354.
18. Adair, G.M., Stallings, R.L., Friend, K.K., and Siciliano, M.J. (1983). *Somat. Cell Genet.* **9**:477–487.
19. Adair, G.M., and Carver, J.H. (1983). *Environ. Mutagen.* **5**:161–175.
20. Saiki, R.K., Scharf, S., Faloona, F., Mullis, K.B., Horn, G.T., Erlich, H.A., and Arnheim, N. (1985). *Science* **230**:1350–1354.
21. Carouthers, A.M., Urlaub, G., Mucha, J., Grunberger, D., and Chasin, L.A. (1989). *Biotechniques* **7**:494–499.
22. Porter, T., Pennington, S.L., Adair, G.M., Nairn, R.S., and Wilson, J.H. (1990). *Nucleic Acids Res.* **18**:5173–5180.
23. Mulligan, R., and Berg, P. (1981). *Proc. Natl. Acad. Sci. U.S.A.* **78**:2072–2076.
24. Maniatis, J., Fritsch, E.F., and Sambrook, J. (1982). *Molecular Cloning: A Laboratory Manual,* (Cold Spring Harbor Press, Cold Spring Harbor, New York).
25. Humphreys, G.O., Willshaw, G.A., and Anderson, E.S. (1975). *Biochim. Biophys. Acta.* **383**:457–463.
26. Nairn, R.S., Adair, G.M., and Humphrey, R.M. (1982). *Mol. Gen. Genet.* **187**:384–390.
27. Nairn, R.S., Humphrey, R.M., and Adair, G.M. (1988). *Int. J. Radiat. Biol.* **53**:249–260.
28. Weinstock, R., Sweet, R., Weiss, M., Cedar, H., and Axel, R. (1978). *Proc. Natl. Acad. Sci. U.S.A.* **75**:1299–1303.

29. Feinberg, A.P., and Vogelstein, B. (1983). *Anal. Biochem.* **132:**6–13.
30. Kucherlapati, R.S., Eves, E.M., Song, K.-Y., Morse, B.S., and Smithies, O. (1984). *Proc. Natl. Acad. Sci. U.S.A.* **81:**3153–3157.
31. Brenner, D.A., Smigocki, A.C., and Camerini-Otero, R.D. (1985). *Mol. Cell. Biol.* **5:**684–691.
32. Wake, C.T., Vernaleone, F., and Wilson, J.H. (1985). *Mol. Cell. Biol.* **5:**2080–2089.
33. Jasin, M., de Villiers, J., Weber, F., and Schaffner, W. (1985). *Cell* **43:**695–703.
34. Rommerskirch, W., Graeber, I., Grassmann, M., and Grassmann, A. (1988). *Nucleic Acids Res.* **16:**941–952.
35. Thomas, K.R., and Capecchi, M.R. (1987). *Cell* **51:**503–512.
36. Szostak, J.W., Orr-Weaver, T.L., and Rothstein, R.J. (1983). *Cell* **33:**25–35.
37. Stanfield, S., and Helinski, D. (1984). *Mol. Cell. Biol.* **4:**173–180.
38. Stanfield, S., and Helinski, D. (1986). *Nucleic Acids Res.* **14:**7823–7838.
39. Doetschman, T., Maeda, N., and Smithies, O. (1988). *Proc. Natl. Acad. Sci. U.S.A.* **85:**8583–8587.
40. Jasin, M., Elledge, S.J., Davis, R.W., and Berg, P. (1990). *Genes Dev.* **4:**157–166.
41. Weber, C.A., Salazar, E.P., Stewart, S.A., and Thompson, L.H. (1990). *EMBO J.* **9:**1437–1447 (1990).
42. Sung, P., Prakash, L., Matson, S.W., and Prakash, S. (1987). *Proc. Natl. Acad. Sci. U.S.A.* **84:**8951–8955.
43. Montelone, B.A., Hoekstra, M.F., and Malone, R.E. (1988). *Genetics* **119:**289–301.
44. Nairn, R.S., Adair, G.M., Christmann, C.B., and Humphrey, R.M. (1991). *Mol. Carcinogen.* **4:**519–526.